

Electronic and Magnetic Properties of Diluted Ferromagnetic Semi Conductor Li (Zn, Mn) P from First-Principles Calculations

L. Hua

Nanjing Normal University Taizhou College, Taizhou 225300, People's Republic of China

Abstract: We have investigated the electronic structure and magnetic properties of Mn-doped LiZnP using density functional theory within the generalized gradient approximation (GGA) +U schemes. We have shown that the ground state magnetic structure of Mn-doped LiZnP is anti ferro magnetic. Li_{Zn} is the most plausible acceptor among several candidates for p-type doping and hole-mediated Zener'sp-d exchange are responsible for the origin of the Li (Zn,Mn) P ferromagnetism.

PACS numbers: 71.15.Mb; 75.20.Hr; 71.20.-b; 75.10.-b

Keywords: A. Mn doped LiZnP; B. GGA+U; C. electronic and magnetic properties; D. first-principles calculation

1. INTRODUCTION

Ferromagnetic systems obtained by doping transition metals into semiconductors have generated extensive studies since early 1990s [1] because of their potential use for spin-sensitive electronics (spintronics) devices. In proto-typical systems based on III-V semiconductors, such as (Ga, Mn)As and (In, Mn)As, substitution of divalent Mn atoms into trivalent Ga or In sites leads to severely limited chemical solubility. Because of this, the specimens are chemically meta stable, available only as thin films [2], and their material quality exhibits high sensitivity on preparation methods and heat treatments[3]. This substitution dopes hole carriers together with magnetic atoms, which prohibits electron doping to obtain n-type systems necessary for formation of spintronics p-n junction devices. To overcome these difficulties, Masek et al [4] theoretically proposed systems based on a I-II-V semiconductor LiZn As, wherein magnetism due to isovalent (Zn, Mn) substitution may be decoupled from carrier doping with excess/deficient Li concentrations. They also suggested that Li (Zn, Mn) As with properly adjusted stoichiometry is a high Curie temperature n-type ferromagnetic semiconductor. Deng et al [5] reported the synthesis of bulk specimens of a ferromagnetic $Li_{1+y}(Zn_{1-x}Mn_x)As$ semiconductor with T_c as high as about 50 K. Ferromagnetism was found only in compounds with excess Li ($y \geq 0.05$). The Li excess specimen exhibit p-type carriers, which may be due to excess Li atoms occupying substitutional Zn sites. Tao et al [6] investigated the ferromagnetic stability of Li(Zn,Mn) As based on the density functional theory. The results indicated that excess Li atoms can be incorporated at interstitial sites near Zn easily and the n-type Li(Zn,Mn) As ferromagnetic semiconductors are achieved. This result is consistent with the reference reported by Maske etal [4] but contrasts with p-type ferromagnetic semiconductors reported by Deng et al [5]. Recently, direct-gap semiconductor LiZn P was also found that it undergoes a ferromagnetic transition upon Mn doping. Ding etal [7] employed NMR techniques to investigate the nature of Mn spins in Li $(Zn_{1-x}Mn_x)P$ ($x = 0.1$). They found that Li $(Zn_{0.9}Mn_{0.1})P$ is a hole-doped semiconductor with T_c about 25 K. They also showed that the Mn spin-spin interactions extend over many unit cells. Deng et al [8] also successfully synthesized bulk crystals of $Li_{1+y}(Zn_{1-x}Mn_x)P$ with $-0.05 \leq y \leq 0.07$ and $x = 0, 0.03, 0.06, 0.1$. It has been shown that doping Mn^{2+} only in $Li_{1+y}(Zn_{1-x}Mn_x)P$, without excess Li doping, will result in a paramagnetic ground state. Only with excess Li being doped, can ferromagnetic ordering develop. They also found that $Li_{1+y}(Zn_{1-x}Mn_x)P, 0 \leq y \leq 0.7$, exhibit p-type behavior, not the n-type behavior. This is

explained by first-principles calculations, which indicate that the excess Li^{1+} ions are thermodynamically favored to occupy the Zn^{2+} sites. Ninget al [9] used muon spin relaxation (μSR) to investigate the magnetic properties of a bulk form diluted ferromagnetic semiconductor $\text{Li}_{1+y}(\text{Zn}_{1-x}\text{Mn}_x)\text{P}$. The μSR results demonstrated the homogenous distribution of Mn^{2+} atoms in $\text{Li}_{1+y}(\text{Zn}_{1-x}\text{Mn}_x)\text{P}$. They did not observe signals arising from Li atoms that enter Zn sites which is inconsistent with Deng et al results. The results also implied that Li (Zn,Mn) P, (Ga,Mn) As, (La,Ba) (Zn,Mn)As O and (Ba,K) (Zn,Mn) $_2$ As $_2$ share a common mechanism for the ferromagnetic exchange interaction. In this paper, we have performed a first-principles density functional theory study on Li(Zn, Mn) P and discussed its electronic and magnetic properties.

2. COMPUTATIONAL METHOD

The first-principles calculations were performed by using density functional theory (DFT) method within the Perdew-Burke-Ernzerh of (PBE) generalized gradient approximation (GGA)[10], implemented in the Viennaab initio Simulation Package (VASP)[11]. The strong correlated correction was considered with GGA+U method [12] to deal with the Mn's 3d electrons. The effective onsite Coulomb interaction parameter (U) and exchange interaction parameter (J) are set to be 4.0 eV and 1.0 eV for Mn's 3d electrons. These values have been tested and used in the previous experimental and theoretical works [13, 14]. For Zn atoms, the strong-correlated correction was not applied as their 3d orbitals are fully occupied. 2s for Li, 3d4s for Zn, 3d4s for Mn and 3s3p for P were treated as valence orbitals in the calculations. The projector augmented wave (PAW) potential [15] and the plane waves cut-off energy of 300 eV were used. For LiZnP unit cell, a Γ -centered Monkhorst-Pack [16] k-point mesh of $5 \times 5 \times 5$ was used and the internal atomic coordinates were relaxed until the force was less than 0.01 eV/Å. For Mn doped LiZnP super cell, a Γ -centered Monkhorst-Pack k-point mesh of $3 \times 3 \times 3$ was used. The criterion for the total energy was set as 10^{-4} eV.

3. RESULTS AND DISCUSSION

LiZnP, the host materials of Li (Zn,Mn)P, has a cubic crystal structure and space group $F\bar{4}3m$ [8], as shown in figure 1.

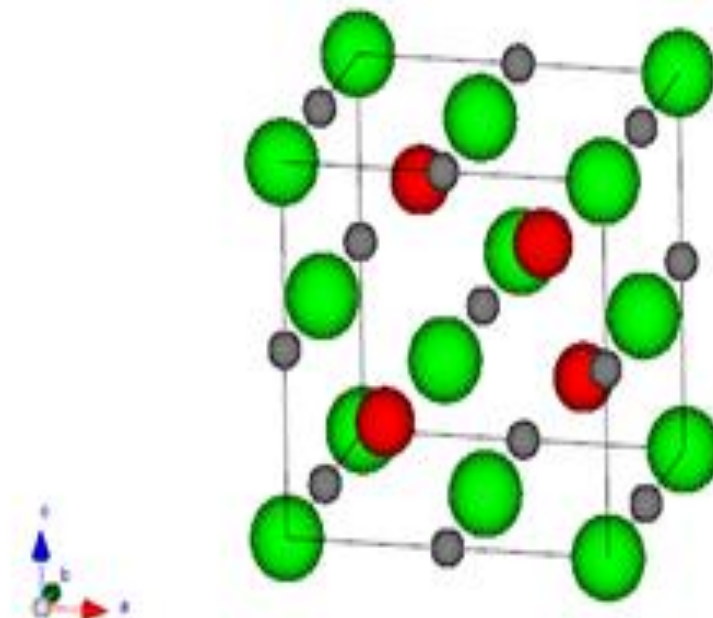


Fig1. The crystal structure of the LiZnP unit cell. The grey spheres are Li, the green spheres are Zn, and the red spheres are P.

Using the experimental lattice constants ($a=5.7564\text{\AA}$)[8] and the numerical internal coordinates, we first investigate the electronic structure of the pure compound LiZnP. In figure 2, the total density of states of the LiZnP are depicted.

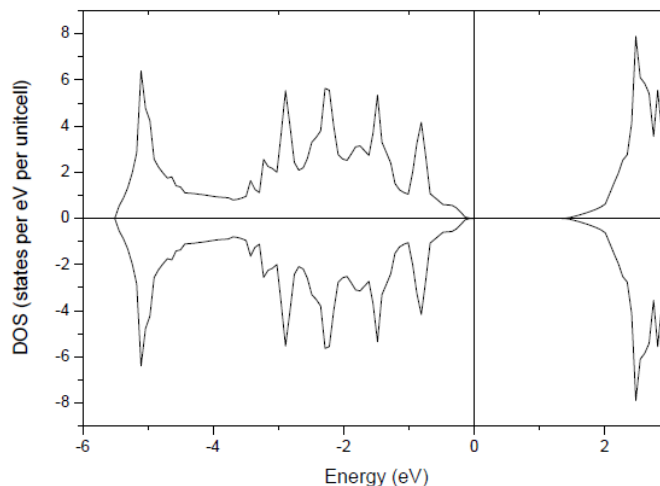


Fig2. The total (black line) density of states of LiZnP per unit cell. The energy zero is taken at the Fermi level and indicated by the vertical line.

This compound is a non-magnetic semiconductor with a calculated band gap at about 1.3 eV which is smaller than the experimental data (2.04 eV) [17]. The reason is the well-known under estimation band gap of DFT. As an indication of the stability of the Mn dopant, the formation energy of Mn_{Zn} is calculated for stoichiometric Li (Zn, Mn) P from [18] $E_f = E_D - E_H - E_{Mn} + E_{Zn}$ where E_D and E_H are the energies of LiZnP with and without defects. E_{Mn} and E_{Zn} are the energies of an isolated manganese atom and a zinc atom, respectively. In figure 3, the calculated formation energies of Mn_{Zn} are plotted as a function of Mn_{Zn} doping for stoichiometric Li (Zn,Mn)P.

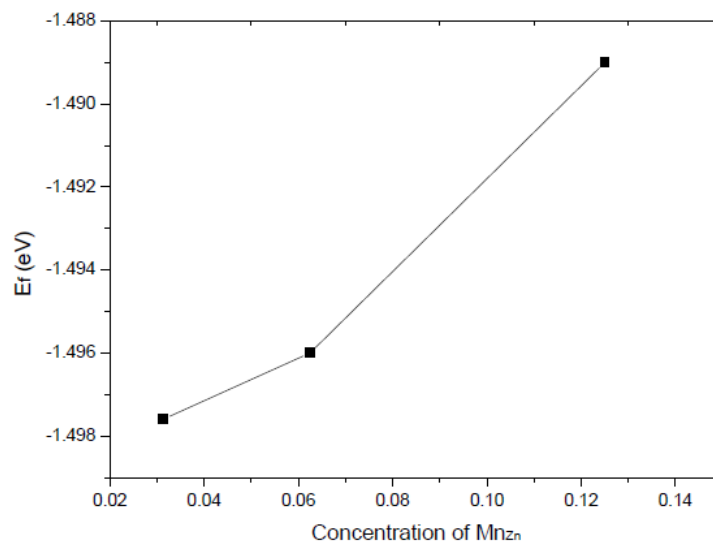


Fig3. The formation energies of Mn_{Zn} as a function of Mn_{Zn} doping for stoichiometric Li (Zn,Mn)P.

Independent of the concentration of Mn_{Zn} doping, the formation energy of Mn_{Zn} is negative, i.e., we find no equilibrium solubility limit for sub substitutional Mn_{Zn} , which indicates that Mn atoms are isovalent nature with Zn atoms. We have used two Mn atoms to substitute two Zn atoms in a $2 \times 2 \times 2$ super cell for constructing Li ($Zn_{0.9375}Mn_{0.0625}$)P. We have calculated five kinds of Mn-Mn pair configuration of different distances.

- (1) The first nearest neighboring two Mn atoms indicating [01],
- (2) The second nearest neighboring two Mn atoms indicating [02],
- (3) The third nearest neighboring two Mn atoms indicating [03],

- (4) The fourth nearest neighboring two Mn atoms indicating [04],
 (5) The fifth nearest neighboring two Mn atoms indicating [05], as shown in figure 4.

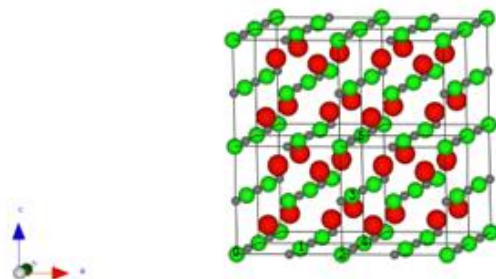


Fig4. The $2 \times 2 \times 2$ super cell of Li (Zn,Mn)P. The configurations of Mn-Mn pair indicate [01], [02], [03], [04] and [05].

Table I. The total energy (eV) of different configuration of ferromagnetic and anti ferromagnetic state of Li ($Zn_{0.9375}Mn_{0.0625}$) P.

Configuration	E_{AFM}	E_{FM}	$E_{FM}-E_{AFM}$
01	-339.7285	-339.6635	0.0650
02	-339.6873	-339.6872	0.0001
03	-339.6929	-339.6853	0.0076
04	-339.6949	-339.6761	0.0188
05	-339.6870	-339.6858	0.0023

Table I lists the total energy of the Li ($Zn_{0.9375}Mn_{0.0625}$) P with ferromagnetic (FM) and Anti ferromagnetic (AFM) state for the five configuration. Our calculations show that the total energy of anti ferromagnetic states are always lower than the ferromagnetic states in the considered Mn-Mn pair configuration. This result means that the ground state of stoichiometric Li ($Zn_{0.9375}Mn_{0.0625}$) P is AFM state. However, this result contradicts the experimental report that Li ($Zn_{0.9}Mn_{0.1}$) P is a hole-doped ferromagnetic semiconductor with T_c about 25 K [7]. We speculate that the different magnetic property between experimental samples and our calculated stoichiometric Li ($Zn_{0.9375}Mn_{0.0625}$) P may come from the defects in the experimental samples. Thus, we have calculated the total energy differences between FM and AFM states versus the concentration of doped carriers and plotted in figure 5. The positive and negative values are for electron and hole doping.

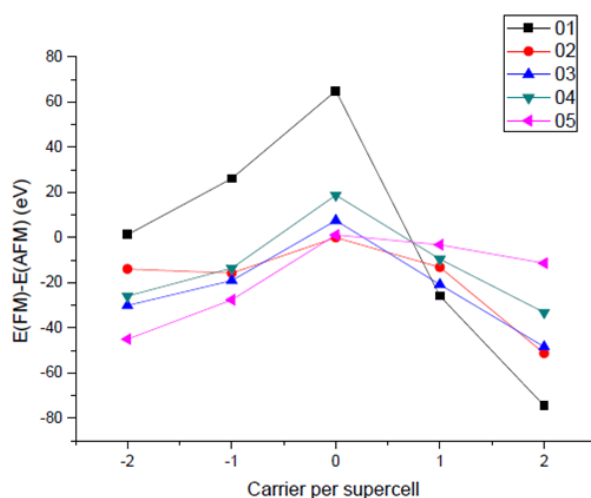


Fig5. The total energy differences between FM and AFM states versus the concentration of doped carriers for five kinds of Mn-Mn pair configurations.

From figure 5, the FM state is stable only with electron carriers for Mn-Mn [01] configuration while hole and electron carriers both can induce a AFM-FM transition for [02], [03], [04], [05] configuration. Considering the homogeneous distribution of Mn^{2+} atoms in $Li_{1+y}(Zn_{1-x}Mn_x)P$ [9], we think that Mn-Mn

Electronic and Magnetic Properties of Diluted Ferromagnetic Semi Conductor Li (Zn, Mn) P from First-Principles Calculations

[02], [03], [04] and [05] configurations should dominate in $\text{Li}_{1-y}(\text{Zn}_{1-x}\text{Mn}_x)\text{P}$. So the formation energy of the p-type or n-type defect will determine the hole or electron carriers induce the AFM-FM transition. The p-type defects include Li vacancy (V_{Li}), Zn vacancy (V_{Zn}), P interstitial (P_{int}) and Li substituting Zn (Li_{Zn}). The n-type defects include Li interstitial (Li_{int}), Zn interstitial (Zn_{int}) and P vacancy (V_{P}).

Table II. The calculated formation energy E_f (eV) of different effects with [02], [03], [04] and [05] Mn-Mn configuration.

	02	03	04	05
V_{Li}	1.596	1.622	1.618	1.618
V_{Zn}	1.359	1.354	1.351	1.297
P_{int}	22.756	22.759	22.757	22.871
Li_{Zn}	-1.184	-1.181	-1.191	-1.202
Li_{int}	8.604	8.045	8.589	7.991
Zn_{int}	19.933	13.427	19.91	13.251
V_{P}	3.558	3.604	3.586	3.56

Table II lists the calculated formation energy E_f of Mn-Mn [02], [03], [04] and [05] configuration with p-type and n-type defect. The Li_{Zn} have the lowest formation energy among these defects and thus create the p-type carriers. This results is consistent with the experimental and theoretical report of Deng et al [8].

Finally, in order to see the origin of the carrier induced ferromagnetism, the density of states of $\text{Li}(\text{Zn}_{0.9375}\text{Mn}_{0.0625})\text{P}$ of Mn-Mn [05] configuration with one Li_{Zn} defect are shown in figure 6.

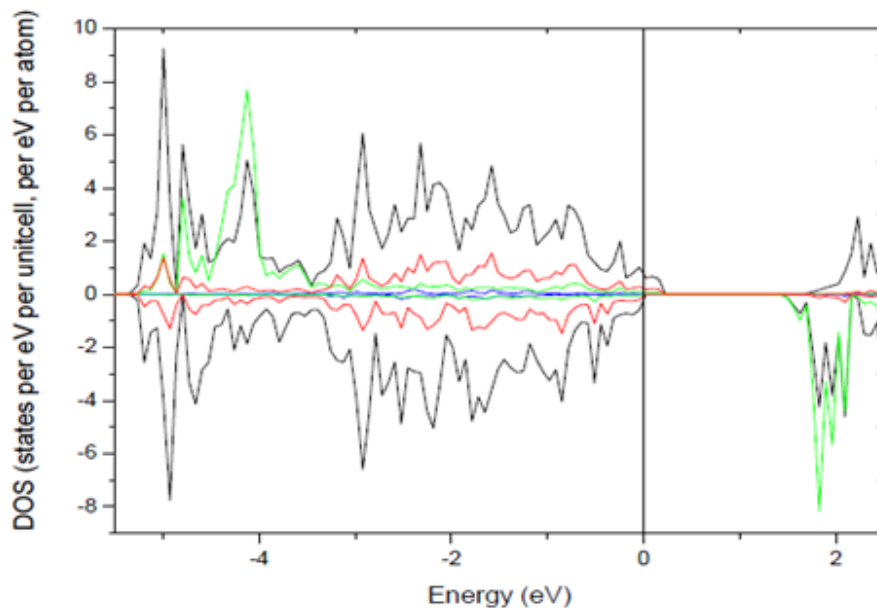


Fig6. The total averaged (black line) and partial density of states of P 3p (red line) of $\text{Li}(\text{Zn}_{0.9375}\text{Mn}_{0.0625})\text{P}$ per unit cell. The partial density of states of Mn 3d (green line) and Li 2s (blue line) per atom. The energy zero is taken at the Fermi level and indicated by the vertical line.

We can see that the contributions from the Li 2s states to the valence bands are negligible. The Li atoms are in the form of cation Li^{1+} and create the p-type carriers by substituting Zn atoms. This result also can be seen from figure 6 that the spin-down states of valence band are full filled while the spin-up partly filled. Thus the hole carriers are introduced into the valence band near the Fermi level, which is mostly composed of the P 3p states. So the delocalized holes have a character of the host states near the top of the valence band and spinpolarized. The main peak in the partial density of states of the spin-up Mn 3d electrons is well below the Fermi level and these states form a local moment. At the same time, the Mn

3d wave functions hybridize with the 3p wave functions of the neighboring P atoms in the interval -4.5 eV to -5.5 eV due to the environment of tetrahedral symmetry T_d . Thus, the ferromagnetic coupling between Mn local moments of Li ($Zn_{0.9375}Mn_{0.0625}$)P is mediated by delocalized band holes via Zener's p-d exchange interaction [19]. The long-range p-d exchange interactions mediated by itinerant holes is also the origin of ferromagnetic coupling in the diluted magnetic semiconductor $(La_{1-x}Ba_x)(Zn_{1-y}Mn_y)AsO$ [20] and $Ba_{1-x}K_x(Zn_{1-y}Mn_y)_2As_2$ [21, 22] from the first-principles calculations, which are also proved by the experiments for the three compounds from Ning et al [9] and Chen et al [23].

4. SUMMARY

In conclusion, we have performed a study of the electronic structure and magnetic properties of Mn-doped LiZnP using density functional theory within the GGA+U schemes. We have shown that the ground state magnetic structure of Mn-doped LiZnP is anti ferromagnetic. Li_{Zn} is the most prospect p-type doping and hole-mediated Zener's p-d exchange are responsible for the origin of ferromagnetism.

REFERENCES

- [1] H. Ohno, A. Shen, F. Matsukura, A. Oiwa, A. Endo, S. Katsumoto, Y. Iye, *Appl. Phys. Lett.* 69, 363 (1996).
- [2] H. Ohno, *Science*. 281, 951 (1998).
- [3] S. J. Potashnik, K. C. Ku, S. H. Chun, J. J. Berry, N. Samarth, P. Schiffer, *Appl. Phys. Lett.* 79, 1495 (2001).
- [4] J. Masek, J. Kudrnovsky, F. Maca, B. L. Gallagher, R. P. Campion, D. H. Gregory, T. Jungwirth, *Phys. Rev. Lett.* 98, 067202 (2007).
- [5] Z. Deng, C. Q. Jin, Q. Q. Liu, X. C. Wang, J. L. Zhu, S. M. Feng, L. C. Chen, R. C. Yu, C. Arguello, T. Goko, F. L. Ning, J. S. Zhang, Y. Y. Wang, A. A. Aczel, T. Munsie, T. J. Williams, G. M. Luke, T. Kakeshita, S. Uchida, W. Higemoto, T. U. Ito, B. Gu, S. Maekawa, G. D. Morris, Y. J. Uemura, *Nat. Commun.* 2, 422 (2011).
- [6] H. L. Tao, Z. H. Zhang, L. L. Pan, M. He, B. Song, *Solid State Commun.* 177, 113 (2014).
- [7] C. Ding, C. Qin, H. Y. Man, T. Imai, F. L. Ning, *Phys. Rev. B*. 88, 041108(R) (2013).
- [8] Z. Deng, K. Zhao, B. Gu, W. Han, J. L. Zhu, X. C. Wang, X. Li, Q. Q. Liu, R. C. Yu, T. Goko, B. Frandsen, L. Liu, J. S. Zhang, Y. Y. Wang, F. L. Ning, S. Maekawa, Y. J. Uemura, C. Q. Jin, *Phys. Rev. B*. 88, 081203(R) (2013).
- [9] F. L. Ning, H. Y. Man, X. Gong, G. X. Zhi, S. L. Guo, C. Ding, Q. Wang, T. Goko, L. Liu, B. A. Frandsen, Y. J. Uemura, H. Luetkens, E. Morenzoni, C. Q. Jin, T. Munsie, G. M. Luke, H. D. Wang, B. Chen, *Phys. Rev. B*. 90, 085123 (2014).
- [10] J. P. Perdew, K. Burke, M. Ernzerhof, *Phys. Rev. Lett.* 77, 3865 (1996).
- [11] G. Kresse, J. Furthmüller, *Phys. Rev. B*. 54, 11169 (1996).
- [12] A. I. Liechtenstein, V. I. Anisimov, J. Zaanen, *Phys. Rev. B*. 52, R5467 (1995).
- [13] J. Okabayashi, A. Kimura, O. Rader, T. Mizokawa, A. Fujimori, T. Hayashi, M. Tanaka, *Phys. Rev. B*. 58, 4211 (1998).
- [14] K. Sato, P. H. Dederichs, H. Katayama, J. Kudrnovsky, *J. Phys.: Condens. Matter*. 16, 5491 (2004).
- [15] P. E. Blöchl, *Phys. Rev. B*. 50, 17953 (1994).
- [16] H. J. Monkhorst, J. D. Pack, *Phys. Rev. B*. 13, 5188 (1976).
- [17] K. Kuriyama, T. Katoh, N. Mineo, *J. Cryst. Growth*. 108, 37 (1991).
- [18] H. Pan, Y. P. Feng, Q. Y. Wu, Z. G. Huang, J. Y. Lin, *Phys. Rev. B*. 77, 125211 (2008).
- [19] K. Sato, L. Bergqvist, J. Kudrnovsky, P. H. Dederichs, O. Eriksson, I. Turek, B. Sanyal, G. Bouzerar, H. Kattayama-Yoshida, V. A. Dinh, T. Fukushima, H. Kizaki, R. Zeller, *Rev. Mod. Phys.* 82, 1633 (2010).
- [20] L. Hua, Q. L. Zhu, J. M. Shen, *Euro. Phys. J. B*. 88, 118 (2015).

- [21] J. T. Yang, S. J. Luo, Y. C. Xiong, Solid. State.Sci. 46,102 (2015).
- [22] H. L. Tao, L. Lin, Z. H. Zhang, M. Hea, B. Song, Comput.Mater. Sci. 98, 93 (2015).
- [23] B. J. Chen, K. Zhao, Z. Deng, W. Han, J. L. Zhu, X.C. Wang, Q. Q. Liu, B. Frandsen, L. Liu, S. Cheung, F.L. Ning, T. J. S. Munsie, T. Medina, G. M. Luke, J. P. Carlo, J. Munevar, Y. J. Uemura, and C. Q. Jin, Phys.Rev. B. 90, 155202 (2014).